A&A 476, 779–790 (2007)
DOI: 10.1051/0004-6361:20078206

Astronomy & Astrophysics

RR Lyrae stars in Galactic globular clusters

VI. The period-amplitude relation

G. Bono[1,2], F. Caputo[1], and M. Di Criscienzo[1,3]

[1] INAF-Osservatorio Astronomico di Roma, via Frascati 33, 00040 Monte Porzio Catone, Italy
e-mail: [bono;caputo;dicriscienzo]@mporzio.astro.it
[2] European Southern Observatory, Karl-Schwarzschild-Str. 2, 85748 Garching bei Munchen, Germany
[3] INAF-Osservatorio Astronomico di Capodimonte, via Moiariello 16, 80131 Napoli, Italy

Received 2 July 2007 / Accepted 18 September 2007

ABSTRACT

Aims. This work uses nonlinear convective models of RR Lyrae stars and evolutionary predictions of low-mass helium burning stellar structures to constrain the properties of cluster and field RR Lyrae variables. In particular, we address two problems: is the Period-Amplitude (PA_V) plane of fundamental (RR_{ab}) variables a good diagnostic for the metal abundance? Is the M_V(RR)-[Fe/H] relation of field and cluster variables linear over the whole metal abundance range of [Fe/H] ~ -2.5 to ~ 0?

Methods. We perform a detailed comparison between theory and observations for fundamental RR Lyrae variables in the solar neighborhood and in both Oosterhoff type I (OoI) and type II (OoII) Galactic globular clusters.

Results. We show that the distribution of cluster RR_{ab} variables in the PA_V plane depends not only on the metal abundance, but also on the cluster Horizontal Branch (HB) morphology. We find that on average the observed pulsation parameter $k_{\rm puls}$ connecting the period to the visual amplitude increases when moving from metal-poor to metal-rich GGCs. However, this parameter shows marginal changes among OoI clusters with intermediate to red HB types and iron abundances $-1.8 \leq$ [Fe/H] ≤ -1.1, whereas its value decreases in OoII clusters with the bluer HB morphology, although these clusters are also the less metal-poor ones of the group. Moreover, at [Fe/H] $= -1.7 \pm 0.1$ the OoI clusters present redder HB types and larger $\langle k_{\rm puls} \rangle$ values than the OoII clusters. The RR_{ab} variables in ω Cen and in the solar neighborhood further support the evidence that the spread in [Fe/H], at fixed $k_{\rm puls}$, is of the order of ± 0.5 dex. Using the results of synthetic HB simulations, we show that the PA_V plane can provide accurate cluster distance estimates. We find that the RR_{ab} variables in OoI and in OoII clusters with very blue HB types obey a well-defined M_V(RR)–$k_{\rm puls}$ relation, while those in OoII clusters with moderately blue HB types present a zero-point that is ~ 0.05 mag brighter. Regarding field variables, we show that with [Fe/H] ≥ -1.0 a unique M_V(RR)–$k_{\rm puls}$ relation can be adopted, independently of the color distribution of the parent HB star population.

Conclusions. Current findings suggest that the PA_V distribution is not a robust diagnostic for the metal abundance of RR_{ab} variables. However, the same observables can be used to estimate the absolute magnitude of globular cluster and field RR_{ab} variables. We show that over the metallicity range $-2.4 \leq$ [Fe/H] ≤ 0.0 the M_V(RR)-[Fe/H] relation is not linear but has a parabolic behavior.

Key words. Galaxy: globular clusters: general – stars: evolution – stars: horizontal-branch – stars: oscillations – stars: variables: RR Lyr

1. Introduction

It has been long recognized that the properties of RR Lyrae variables provide firm constraints on several important aspects of stellar evolution and cosmology. The calibration of the absolute visual magnitude M_V(RR) as a function of the iron-to-hydrogen content [Fe/H] is generally used for distance determinations in the Local Group and the RR Lyrae-based distances provide an independent test for the Cepheid distance scale in nearby galaxies (Magellanic Clouds, M 31, dwarf spheroidal galaxies) and for the calibration of secondary distance indicators such as the globular cluster luminosity function in more distant galaxies (see e.g. Di Criscienzo et al. 2006, and references therein). Moreover, the distance of RR Lyrae stars observed in globular clusters is a fundamental step to determine the absolute magnitude of the cluster main-sequence turn-off, which is the classical "clock" to estimate the age of these ancient stellar systems.

Together with this traditional role for distance determinations, since the pioneering investigation by Preston (1959) it has also been suggested that the location of fundamental mode variables (RR_{ab}) in the Period-Amplitude (PA_V) plane, i.e., in the so-called Bailey diagram, depends on the metal abundance. Among the more recent papers, we mention Alcock et al. (2000) who used the visual amplitude of RR_{ab} stars in the globular clusters M 15 ([Fe/H] $= -2.1$), M 3 ([Fe/H] $= -1.6$) and M5 ([Fe/H] $= -1.4$) to obtain the calibration

$$[{\rm Fe/H}]_{\rm A} = -2.60 - 8.85 \log P_{ab} - 1.33 A_V \quad (1)$$

and Sandage (2004) who determined

$$[{\rm Fe/H}]_{\rm S} = -2.15 - 7.99 \log P_{ab} - 1.45 A_V \quad (2)$$

from field variables with spectroscopic [Fe/H] measurements. Although these Period-Metallicity-Amplitude relations present a large intrinsic indeterminacy of ~ 0.35 dex, they were used by Alcock et al. (2000) to estimate a median metal content of [Fe/H] ~ -1.6 for a very large sample of RR_{ab} stars in the bar of the Large Magellanic Cloud (LMC), by Brown et al. (2004) to derive a mean metallicity of [Fe/H] $= -1.8 \pm 0.3$ for the 29 RR_{ab} variables they identified in a halo field of M 31, and

by Kinemuchi et al. (2006) to study the properties of RR Lyrae stars in the solar neighborhood.

The suggested dependence of the Bailey diagram on the metal abundance accounts for the observational evidence that RR$_{ab}$ stars in Oosterhoff type II globular clusters tend to have, for a given amplitude, longer periods than those in Oosterhoff type I clusters. According to the average period $\langle P_{ab} \rangle$ of their *ab*-type variables, globular clusters are conventionally classified into two Oosterhoff groups. The Oosterhoff type I (OoI) group includes metal-intermediate clusters with $\langle P_{ab} \rangle \sim 0.55$ days, while the Oosterhoff type II (OoII) group includes metal-poor clusters with $\langle P_{ab} \rangle \sim 0.65$ days. However, OoII clusters show bluer horizontal branch (HB) star distributions than OoI clusters. Therefore the PA_V diagram, as already suggested by Clement & Shelton (1999), migth not depend on the metal abundance but on the evolutionary status of RR Lyrae stars.

From a theoretical point of view, it is widely accepted that the pulsation period P is physically governed by the von Ritter relation $P\rho^{1/2} = Q$ (ρ is the stellar density and Q the pulsation constant) which yields that the pulsation period is function of the pulsator mass M, luminosity L, and effective temperature T_e. Since the earlier linear and adiabatic pulsation models, the $P = f(M, L, T_e)$ relation, the so-called van Albada & Baker (1971, 1973) relation, has been fundamental to several investigations focused on the estimate of RR Lyrae mass and luminosity. However, accurate predictions concerning the luminosity and the radial velocity variations along the pulsation cycle, and their dependence on the pulsation structural parameters, became available only with the modern nonlinear, convective approach (Stellingwerf 1984).

The purpose of the present investigation is to use detailed sets of nonlinear, convective models for fundamental (F) pulsators computed by our group (see Marconi et al. 2003, Paper II; Di Criscienzo et al. 2004, Paper III, and references therein) to investigate the PA_V relation for RR$_{ab}$ variables. The theoretical scenario is discussed in Sect. 2, while Sect. 3 deals with the comparison with observations. The role of the Period-Amplitude diagram in the distance estimate of RR$_{ab}$ variables is presented in Sect. 4 and the conclusions close the paper.

2. The physical meaning of the PA_V relation

The adopted pulsation models have been computed with the nonlinear convective, hydrodynamical code which has been described in previous investigations (see Papers II, III, and references therein) and it will not be further discussed. The grid of models covers a wide range in stellar mass, luminosity, and chemical composition (see Table 1) and the bolometric light curves of the models have been transformed into the observational plane by adopting the bolometric corrections and color-temperature transformations provided by Castelli et al. (1997a,b). This approach allows us to derive light-curve amplitudes A_i and mean absolute magnitudes, either intensity-weighted $\langle M_i \rangle$ or magnitude-weighted (M_i), for the various photometric bands.

The entire set of models pulsating in the fundamental mode shows a linear correlation between the bolometric amplitude and the pulsation period (logarithmic scale) in the sense that the amplitude decreases from short to long periods, at fixed mass and luminosity. Moreover, we found that the luminosity amplitude, at fixed period, increases as the stellar luminosity increases or as the stellar mass decreases, but to a lesser extent (see Fig. 3 in Paper II). The pulsation limit cycle stability is also governed by the efficiency of convection as a flux carrier

Table 1. Main parameters of the pulsation models used in this paper.

Y	Z	$M/M_\odot$	$\log L/L_\odot$
0.24	0.0001	0.80	1.72, 1.81, 1.91
		0.75	1.61, 1.72, 1.81
		0.70	1.72
		0.65	1.61
0.24	0.0004	0.70	1.61, 1.72, 1.81
0.24	0.001	0.75	1.71
		0.65	1.51, 1.61, 1.72
0.255	0.006	0.58	1.55, 1.65, 1.75

in the stellar envelope, and in turn on the value of the mixing-length parameter l/H_p adopted to close the system of convective and hydrodynamical equations. Note that the depth of the convective region increases when moving from higher to lower effective temperatures and that convection is the physical mechanism that quenches pulsation instability. As a consequence, the RR Lyrae models at constant stellar mass and luminosity show that an increase in the mixing-length parameter from $l/H_p = 1.5$ to 2.0 causes a systematic decrease (∼100 K) in the effective temperature of the first overtone blue edge (FOBE) and the simultaneous increase in the effective temperature of both the blue edge (FBE, ∼100 K) and the red edge (FRE, ∼300 K) of fundamental pulsation. As a whole, the increase in the efficiency of the convective transport causes a narrowing of the width in temperature of the instability strip. On the other hand, the amplitude of fundamental pulsators reaches its maximum value close to the FBE and attains vanishing values close to the FRE. This yields that different assumptions concerning the mixing-length parameter affect the region of the instability strip where fundamental pulsators are pulsationally unstable, and in turn affect both the zero-point and the slope of the predicted Period-Amplitude relation.

Using the intensity-averaged $\langle M_V \rangle$ magnitudes of fundamental pulsators with $Z = 0.0001$–0.006, we find that the correlation between pulsation period, visual amplitude, magnitude, and mass (in solar units) is given by

$$\log P_{ab} = 0.136 - 0.189A_V - 0.385\langle M_V \rangle - 0.30 \log M \quad (3)$$

for $l/H_p = 1.5$, and

$$\log P_{ab} = 0.027 - 0.142A_V - 0.385\langle M_V \rangle - 0.35 \log M \quad (4)$$

for $l/H_p = 2.0$, where the rms dispersion of the fit is 0.025 dex. Let us emphasize that in these relations the pulsator mass and luminosity are free parameters.

According to these relations, the RR$_{ab}$ distribution in the PA_V diagram is described by the *pulsation* parameter

$$k(1.5)_{puls} = 0.136 - \log P_{ab} - 0.189A_V$$

or

$$k(2.0)_{puls} = 0.027 - \log P_{ab} - 0.142A_V,$$

which in turn depends on the pulsator *evolutionary* properties as

$$k(1.5)_{ev} = 0.385\langle M_V \rangle + 0.30 \log M$$

and

$$k(2.0)_{ev} = 0.385\langle M_V \rangle + 0.35 \log M.$$

At variance with the pulsational parameters $k(1.5)_{puls}$ and $k(2.0)_{puls}$, the values of the evolutionary ones $k(1.5)_{ev}$ and $k(2.0)_{ev}$ cannot be directly estimated from observations.

Table 2. Selected results of SHB simulations with $Z \leq 0.006$. For each metal content Z and mean mass of HB stars M(HB), we list the predicted mean values of the HB type and of the RR Lyrae mass, absolute magnitude and k_{ev} parameters, together with the rms dispersion about the mean. The masses are in solar units.

M(HB)	⟨HB⟩	⟨M(RR)⟩	⟨M_V(RR)⟩	⟨$k(1.5)_{ev}$⟩	⟨$k(2.0)_{ev}$⟩
		$Z = 0.0001$, $Y = 0.23$			
0.68	$+0.96 \pm 0.01$	0.70 ± 0.02	0.35 ± 0.02	0.088 ± 0.012	0.080 ± 0.012
0.70	$+0.90 \pm 0.02$	0.71 ± 0.03	0.38 ± 0.01	0.101 ± 0.006	0.094 ± 0.006
0.72	$+0.83 \pm 0.02$	0.73 ± 0.03	0.41 ± 0.01	0.115 ± 0.004	0.108 ± 0.006
0.74	$+0.74 \pm 0.02$	0.75 ± 0.03	0.42 ± 0.01	0.125 ± 0.002	0.119 ± 0.002
0.76	$+0.62 \pm 0.03$	0.77 ± 0.03	0.44 ± 0.01	0.134 ± 0.002	0.128 ± 0.002
0.78	$+0.43 \pm 0.03$	0.79 ± 0.03	0.45 ± 0.01	0.143 ± 0.002	0.138 ± 0.002
0.80	$+0.15 \pm 0.01$	0.81 ± 0.03	0.46 ± 0.01	0.149 ± 0.002	0.144 ± 0.002
0.82	-0.09 ± 0.02	0.82 ± 0.02	0.46 ± 0.01	0.152 ± 0.002	0.148 ± 0.002
0.84	-0.19 ± 0.02	0.84 ± 0.02	0.46 ± 0.01	0.152 ± 0.002	0.148 ± 0.002
		$Z = 0.0003$, $Y = 0.23$			
0.64	$+0.97 \pm 0.01$	0.66 ± 0.02	0.36 ± 0.04	0.084 ± 0.030	0.075 ± 0.030
0.66	$+0.91 \pm 0.01$	0.68 ± 0.02	0.44 ± 0.02	0.117 ± 0.008	0.109 ± 0.008
0.68	$+0.78 \pm 0.01$	0.70 ± 0.02	0.49 ± 0.01	0.142 ± 0.004	0.134 ± 0.004
0.70	$+0.52 \pm 0.02$	0.71 ± 0.02	0.53 ± 0.01	0.161 ± 0.002	0.154 ± 0.002
0.72	$+0.11 \pm 0.03$	0.73 ± 0.02	0.55 ± 0.01	0.170 ± 0.002	0.163 ± 0.002
0.74	-0.29 ± 0.03	0.74 ± 0.02	0.56 ± 0.01	0.174 ± 0.002	0.168 ± 0.002
0.76	-0.60 ± 0.02	0.75 ± 0.02	0.56 ± 0.01	0.176 ± 0.002	0.170 ± 0.002
0.78	-0.82 ± 0.01	0.76 ± 0.02	0.55 ± 0.01	0.176 ± 0.002	0.170 ± 0.002
		$Z = 0.0006$, $Y = 0.23$			
0.62	$+0.97 \pm 0.01$	0.65 ± 0.02	0.37 ± 0.03	0.087 ± 0.026	0.078 ± 0.026
0.64	$+0.89 \pm 0.01$	0.66 ± 0.02	0.48 ± 0.02	0.131 ± 0.012	0.122 ± 0.012
0.66	$+0.70 \pm 0.02$	0.68 ± 0.02	0.53 ± 0.01	0.155 ± 0.006	0.147 ± 0.006
0.68	$+0.28 \pm 0.03$	0.69 ± 0.02	0.57 ± 0.01	0.170 ± 0.002	0.162 ± 0.002
0.70	-0.24 ± 0.02	0.70 ± 0.02	0.58 ± 0.01	0.176 ± 0.002	0.168 ± 0.002
0.72	-0.69 ± 0.02	0.70 ± 0.02	0.59 ± 0.01	0.180 ± 0.002	0.172 ± 0.002
0.74	-0.91 ± 0.01	0.71 ± 0.02	0.59 ± 0.01	0.182 ± 0.002	0.174 ± 0.002
0.76	-0.98 ± 0.01	0.72 ± 0.02	0.59 ± 0.01	0.183 ± 0.002	0.176 ± 0.002
		$Z = 0.001$, $Y = 0.23$			
0.60	$+0.98 \pm 0.01$	0.64 ± 0.01	0.41 ± 0.06	0.099 ± 0.040	0.089 ± 0.040
0.62	$+0.89 \pm 0.01$	0.65 ± 0.01	0.51 ± 0.03	0.141 ± 0.018	0.132 ± 0.018
0.64	$+0.64 \pm 0.02$	0.66 ± 0.01	0.58 ± 0.02	0.170 ± 0.008	0.161 ± 0.008
0.66	$+0.11 \pm 0.02$	0.67 ± 0.01	0.61 ± 0.01	0.181 ± 0.002	0.172 ± 0.002
0.68	-0.44 ± 0.03	0.67 ± 0.01	0.62 ± 0.01	0.188 ± 0.002	0.180 ± 0.002
0.70	-0.80 ± 0.02	0.68 ± 0.01	0.63 ± 0.01	0.192 ± 0.002	0.184 ± 0.002
0.72	-0.96 ± 0.01	0.68 ± 0.01	0.63 ± 0.01	0.194 ± 0.002	0.186 ± 0.002
		$Z = 0.003$, $Y = 0.23$			
0.56	$+0.97 \pm 0.01$	0.60 ± 0.01	0.56 ± 0.07	0.149 ± 0.040	0.138 ± 0.040
0.58	$+0.84 \pm 0.02$	0.61 ± 0.01	0.68 ± 0.03	0.198 ± 0.020	0.187 ± 0.020
0.60	$+0.40 \pm 0.03$	0.61 ± 0.01	0.73 ± 0.01	0.218 ± 0.004	0.208 ± 0.004
0.62	-0.25 ± 0.03	0.62 ± 0.01	0.76 ± 0.01	0.227 ± 0.004	0.217 ± 0.004
0.64	-0.77 ± 0.02	0.62 ± 0.01	0.77 ± 0.01	0.234 ± 0.006	0.223 ± 0.006
0.66	-0.97 ± 0.01	0.62 ± 0.01	0.78 ± 0.01	0.236 ± 0.008	0.226 ± 0.008
		$Z = 0.006$, $Y = 0.245$			
0.54	$+0.97 \pm 0.01$	0.58 ± 0.01	0.63 ± 0.10	0.172 ± 0.070	0.160 ± 0.070
0.56	$+0.79 \pm 0.02$	0.58 ± 0.01	0.80 ± 0.03	0.237 ± 0.012	0.226 ± 0.012
0.58	$+0.29 \pm 0.03$	0.59 ± 0.01	0.84 ± 0.01	0.254 ± 0.008	0.243 ± 0.008
0.60	-0.42 ± 0.02	0.59 ± 0.01	0.86 ± 0.01	0.261 ± 0.004	0.250 ± 0.004
0.62	-0.86 ± 0.01	0.59 ± 0.01	0.88 ± 0.01	0.270 ± 0.006	0.258 ± 0.006
0.64	-0.98 ± 0.01	0.59 ± 0.01	0.88 ± 0.03	0.270 ± 0.032	0.259 ± 0.032

However, all the synthetic horizontal branches (SHB) simulations (see, e.g., Demarque et al. 2000; Catelan et al. 2004; Cassisi et al. 2004, Paper IV) agree in suggesting that, for a fixed metallicity, the average mass of HB stars in the RR Lyrae region decreases when moving from red to blue HB morphologies, whereas the average luminosity presents an opposite trend. Furthermore, for a fixed HB morphology, an increase in the metal content causes a decrease in the same intrinsic parameters.

Using the SHBs computed in Paper IV for various chemical compositions, we show in Table 2 some selected predictions based on SHB simulations in which the number of predicted RR Lyrae stars approaches ∼2% of the global HB star population. For each assumed chemical composition and mean mass[1] M(HB) of HB stars, we give the average HB type[2] and the predicted mean values of the RR Lyrae mass, absolute magnitude, and k_{ev} parameter, together with the rms dispersion about the

[1] The SHBs have been computed by assuming a Gaussian random distribution of HB masses centered on M(HB) and with a standard deviation $\sigma \sim 0.02\ M_{\odot}$.

[2] This parameter is the ratio $(B-R)/(B+V+R)$ between the numbers of HB stars to the blue (B), within (V) and to the red (R) of the RR Lyrae instability strip (Lee 1990).

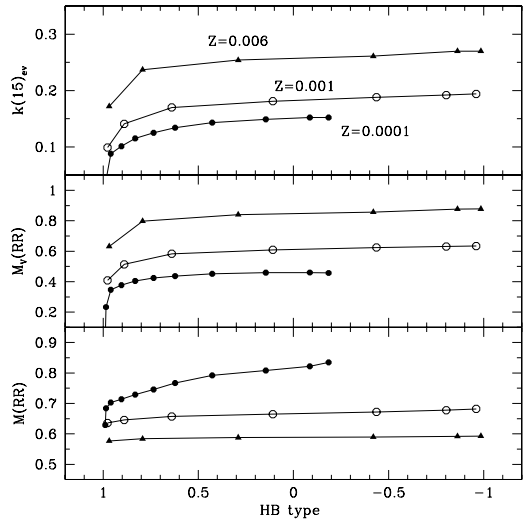

Fig. 1. *From bottom to top*: the average mass M(RR) in solar units, the absolute visual magnitude M_V(RR), and the evolutionary parameter $k(1.5)_{\rm ev}$ as a function of the HB type. Current predictions rely on a set of SHB simulations discussed in Paper IV.

mean. Note that these mean values are derived by averaging the results of 10 different simulations.

Data listed in Table 2 (see also Fig. 1) reveal four substantial points:

1. the mass range of the predicted RR Lyrae decreases with increasing metal content, when moving from very blue to very red HB type distributions;
2. the $k_{\rm ev}$ parameter, at fixed metallicity, attains rather constant values from red to moderately blue HB morphology (i.e., for HB type ranging from $\sim$−0.9 to $\sim$+0.5), whereas it significantly decreases for the bluer populations;
3. the $k_{\rm ev}$ parameter, at constant HB type, increases when moving from low to high metal abundances. However, for HB $\geq$ +0.9 the metallicity effect tends to vanish;
4. the size of this metallicity effect varies with the metallicity range. In particular, for HB type $\sim$0 we get $\Delta k(1.5)_{\rm ev} \sim 0.03$ for $0.0001 \leq Z \leq 0.001$ and $\Delta k(1.5)_{\rm ev} \sim 0.08$ for $0.001 \leq Z \leq 0.006$.

In summary, the constraints on $k_{\rm ev}$ provided by the evolutionary predictions suggest that the PA_V distribution of RR$_{ab}$ stars in globular clusters depends *both on the cluster metal abundance and on the HB morphology*.

3. Observed PA_V diagrams

3.1. Galactic globular clusters

For the RR Lyrae stars in Galactic globular clusters for which the visual amplitude A_V is available in the literature, Table 3 gives the observed HB type (Harris 2003)[3], the average period of RR_{ab} variables and the iron-to-hydrogen content [Fe/H]$_K$ on the Kraft & Ivans (2003) metallicity scale. For ω Cen, whose RR Lyrae stars are characterized by a wide spread in metal abundance, we list the average value ([Fe/H] = -1.62 ± 0.27) based on Rey et al. (2000) data and the HB type determined by Piersimoni et al. (2007, in preparation). As far as NGC 6441 is concerned, the HB type has been determined by Catelan (2005) although this cluster shows a very unusual HB extending from a stubby red to a very blue component (Rich et al. 1997). Moreover, the periods of the observed RR$_{ab}$ variables are too long for the current cluster metallicity, thus hampering a safe Oosterhoff classification (see e.g. Pritzl et al. 2001).

[3] http://physwww.physics.mcmaster.ca/%7Eharris/mwgc.dat)

Table 3. Selected parameters for Galactic globular clusters: HB type, average period of *ab*-type RR Lyrae stars and iron-to-hydrogen content [Fe/H]$_K$ according to the Kraft & Ivans (2003) metallicity scale. For ω Cen, we list the average [Fe/H]$_R$ value from Rey et al. (2000) data.

Name	HB	$\langle \log P_{ab} \rangle$	[Fe/H]$_K$
Oosterhoff type II			
N4590 (M68)	+0.44	−0.201	−2.43
N6426	+0.58	−0.153	−2.43
N7078 (M 15)	+0.67	−0.189	−2.42
N5053	+0.52	−0.174	−2.41
N6341 (M92)	+0.91	−0.195	−2.38
N5466	+0.58	−0.172	−2.22
N5024 (M53)	+0.81	−0.189	−2.02
N6809 (M55)	+0.87	−0.181	−1.85
N6333 (M9)	+0.87	−0.203	−1.79
N7089 (M2)	+0.96	−0.168	−1.56
Oosterhoff type I			
N4147	+0.55	−0.282	−1.79
I4499	+0.11	−0.238	−1.60
N6934	+0.25	−0.252	−1.59
N3201	+0.08	−0.252	−1.56
N5272 (M 3)	+0.08	−0.257	−1.50
N7006	−0.28	−0.246	−1.48
N6715 (M54)	+0.75	−0.237	−1.47
N6981 (M72)	+0.14	−0.256	−1.42
N6229	+0.24	−0.270	−1.41
N6864 (M75)	−0.07	−0.231	−1.29
N5904 (M5)	+0.31	−0.263	−1.26
N1851	−0.36	−0.241	−1.19
N6121 (M4)	−0.06	−0.275	−1.15
N6362	−0.58	−0.265	−1.15
N6723	−0.08	−0.262	−1.11
N6171 (M107)	−0.73	−0.272	−1.10
Peculiar clusters			
N5139 (ω Cen)	+0.92	−0.189	−1.62
N6441	−0.73	−0.132	−0.85

Figure 2 shows the cluster HB type as a function of the metal content [Fe/H]$_K$. Note that even the selected sample of RR Lyrae-rich globular clusters presents the so-called *second parameter* problem: in order to account for the observed HB morphology, together with the metal abundance, a further intrinsic parameter is required. However, we also note that OoI and OoII clusters seem to follow quite different behaviors: the HB morphology of the OoI clusters becomes bluer as the metal content decreases, whereas for the latter group the HB morphology becomes bluer as the cluster becomes more metal-rich. As a consequence, the OoII clusters with very blue HB morphology, including ω Cen, appear to be the "natural" extension of OoI clusters to lower metal abundances.

Figure 3 shows the PA_V diagram of the observed RR$_{ab}$ stars in OoII (top panel) and OoI (bottom panel) clusters. The variables in ω Cen and in NGC 6441 have not been included in this figure and will be discussed separately. The solid line in the top panel is the ridge line of variables in OoII clusters and it was drawn by adopting the predicted slope $\delta \log P_F / \delta A_V = -0.189$ (see Eq. (3)). The same line is also plotted in the bottom panel to emphasize that RR Lyrae stars in OoI clusters present systematically shorter period, at fixed pulsation amplitude.

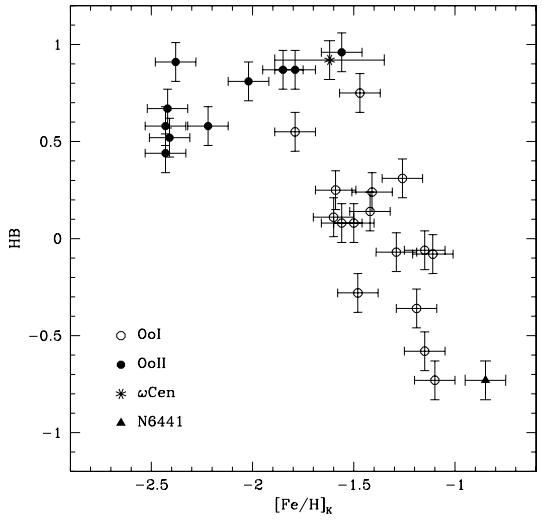

Fig. 2. The HB type versus the metal content $[Fe/H]_K$ for Oosterhoff type II (OoII, filled circles) and Oosterhoff type I (OoI, open circles) Galactic globular clusters. The error bars have been estimated by assuming ϵ(HB) = ±0.1 and $\epsilon[Fe/H]_K$ = ±0.1 For ω Cen (asterisk), we plot the average value $[Fe/H]_R = -1.62 \pm 0.27$ derived by Rey et al. (2000).

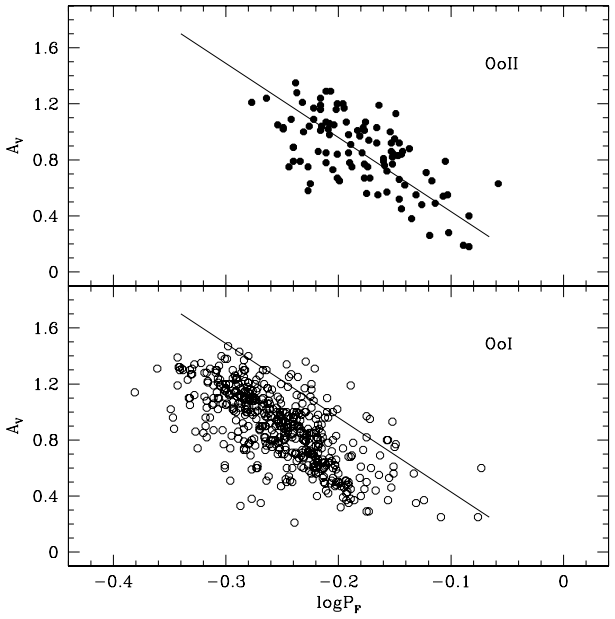

Fig. 3. Visual amplitude versus period for RR$_{ab}$ stars in Oosterhoff type II (OoII, *top panel*) and Oosterhoff type I (OoI, *bottom panel*) globular clusters. The solid line shows the ridge line of variables in OoII clusters and is based on the predicted slope $\delta \log P_F / \delta A_V = -0.189$.

Based on the data plotted in Fig. 3, we derive the average $\langle k(1.5)_{\rm puls} \rangle$ and $\langle k(2.0)_{\rm puls} \rangle$ values listed in Table 4 together with their standard deviations. Figures 4 and 5 show these parameters versus the cluster HB type and the metal content $[Fe/H]_K$, respectively. In the latter figure, the OoII clusters are also selected according to the HB morphology.

As a whole, we find that:

– among the OoI clusters, which have metal abundances from [Fe/H] = −1.8 to −1.1 and HB types redder than +0.75, neither the $\langle k(1.5)_{\rm puls} \rangle$ nor the $\langle k(2.0)_{\rm puls} \rangle$ parameter show significant variation with [Fe/H] or HB type;

Table 4. Mean $k(1.5)_{\rm puls}$ and $k(2.0)_{\rm puls}$ values for RR$_{ab}$ stars in Galactic globular clusters.

Name	HB	$[Fe/H]_K$	$\langle k(1.5)_{\rm puls} \rangle$	$\langle k(2.0)_{\rm puls} \rangle$
		Oosterhoff type II		
N4590	+0.44	−2.43	0.181 ± 0.026	0.118 ± 0.024
N6426	+0.58	−2.43	0.131 ± 0.018	0.068 ± 0.017
N7078	+0.67	−2.42	0.184 ± 0.030	0.118 ± 0.030
N5053	+0.52	−2.41	0.163 ± 0.045	0.095 ± 0.036
N6341	+0.91	−2.38	0.144 ± 0.026	0.089 ± 0.021
N5466	+0.58	−2.22	0.116 ± 0.041	0.063 ± 0.031
N5024	+0.81	−2.02	0.137 ± 0.029	0.080 ± 0.029
N6809	+0.87	−1.85	0.132 ± 0.024	0.077 ± 0.018
N6333	+0.87	−1.79	0.130 ± 0.017	0.080 ± 0.016
N7089	+0.96	−1.56	0.132 ± 0.031	0.073 ± 0.033
		Oosterhoff type I		
N4147	+0.55	−1.79	0.215 ± 0.021	0.164 ± 0.025
I4499	+0.11	−1.60	0.209 ± 0.036	0.149 ± 0.033
N6934	+0.25	−1.59	0.219 ± 0.037	0.160 ± 0.031
N3201	+0.08	−1.56	0.211 ± 0.042	0.154 ± 0.034
N5272	+0.08	−1.50	0.194 ± 0.032	0.142 ± 0.027
N7006	−0.28	−1.48	0.222 ± 0.027	0.160 ± 0.023
N6715	+0.75	−1.47	0.220 ± 0.037	0.157 ± 0.032
N6981	+0.14	−1.42	0.244 ± 0.035	0.180 ± 0.033
N6229	+0.24	−1.41	0.219 ± 0.024	0.164 ± 0.019
N6864	−0.07	−1.29	0.201 ± 0.059	0.141 ± 0.055
N5904	+0.31	−1.26	0.211 ± 0.049	0.156 ± 0.048
N1851	−0.36	−1.19	0.198 ± 0.040	0.141 ± 0.035
N6121	−0.06	−1.15	0.184 ± 0.030	0.142 ± 0.034
N6362	−0.58	−1.15	0.218 ± 0.030	0.162 ± 0.029
N6723	−0.08	−1.11	0.210 ± 0.049	0.155 ± 0.042
N6171	−0.73	−1.10	0.239 ± 0.043	0.179 ± 0.041
		Peculiar clusters		
N5139	+0.92	−1.62	0.150 ± 0.043	0.092 ± 0.052
N6441	−0.73	−0.85	0.106 ± 0.025	0.048 ± 0.025

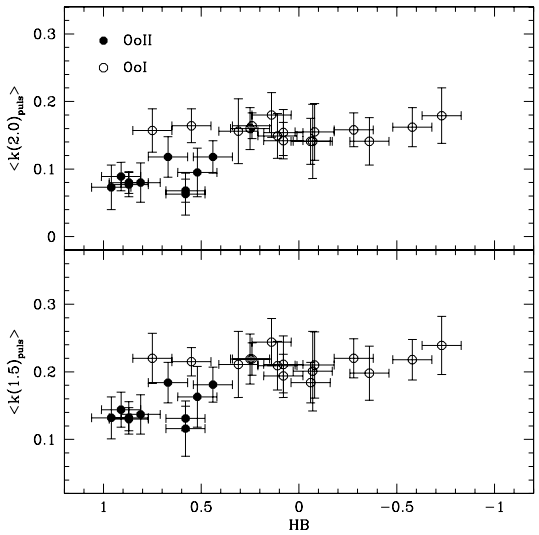

Fig. 4. The average $\langle k(1.5)_{\rm puls} \rangle$ (*bottom panel*) and $\langle k(2.0)_{\rm puls} \rangle$ (*top panel*) values for RR$_{ab}$ stars in Oosterhoff type I (OoI, open circles) and Oosterhoff type II (OoII, filled circles) globular clusters plotted as a function of the cluster HB type.

– among the OoII clusters, which have metal abundances ranging from [Fe/H] = −2.4 to −1.6 and HB types bluer than +0.44, both $\langle k(1.5)_{\rm puls} \rangle$ and $\langle k(2.0)_{\rm puls} \rangle$ present a mild decrease for the clusters with bluer HB morphologies, although they are also the less metal-poor ones of the group;

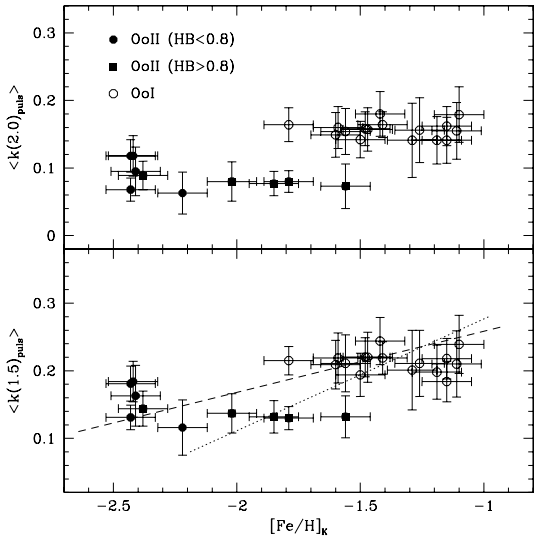

Fig. 5. The average $\langle k(1.5)_{\rm puls}\rangle$ (*bottom panel*) and $\langle k(2.0)_{\rm puls}\rangle$ (*top panel*) values for RR$_{ab}$ stars in Oosterhoff type I (OoI, open circles) and Oosterhoff type II (OoII) globular clusters as a function of metal abundance. The filled circles mark OoII clusters with HB type ranging from red to moderately blue, while the filled squares refer to those with very blue HB type. The dashed and the dotted lines in the bottom panel display two different choices in the selection of the calibrating clusters. See text for more details.

– for [Fe/H] = -1.7 ± 0.1, where both OoI and OoII clusters are observed, the former clusters have redder HB types *and* larger $\langle k_{\rm puls}\rangle$ values than the latter ones.

Bearing in mind the above discussion on the $k_{\rm ev}$ values listed in Table 2, the Bailey diagram of the RR$_{ab}$ stars observed in Galactic globular clusters agrees with the evolutionary prescriptions and does not support the use of a unique PA_V relation for robust metal abundance determinations. The linear fit over the entire dataset plotted in the bottom panel of Fig. 5 gives [Fe/H] $\sim -3.1 + 7.7k(1.5)_{\rm puls}$. This relation would predict the RR$_{ab}$ metallicity with a large average uncertainty of ∼0.4 dex. The intrinsic error becomes even greater if the adopted empirical calibration relies on individual clusters. The use of OoI clusters together with OoII clusters with moderately blue HB morphology yields [Fe/H] $\sim -3.9 + 11.1k(1.5)_{\rm puls}$ (see the dashed line in the bottom panel of Fig. 5), while the use of OoI clusters together with OoII clusters with very blue HB morphology yields (see the dotted line) [Fe/H] $\sim -2.7 + 5.8k(1.5)_{\rm puls}$. Note that the application of the former relation to RR$_{ab}$ variables in OoII clusters with very blue HB stellar populations would underestimate by ∼0.7 dex the metallicity of these variables, while the application of the latter relation to RR$_{ab}$ variables in OoII clusters with moderately blue HB stellar populations would overestimate by ∼0.5 dex the metallicity of the these variables.

3.2. NGC 6441 and ω Cen

Figure 6 shows the PA_V diagram of *ab*-type variables in NGC 6441 and ω Cen together with the ridge line of OoII variables (see Fig. 3). Data plotted in this figure support the evidence that all the RR$_{ab}$ stars in NGC 6441 behave as OoII variables (see also the $\langle k(1.5)_{\rm puls}\rangle$ and $\langle k(2.0)_{\rm puls}\rangle$ values listed in Table 4) suggesting that the RR Lyrae metal abundance is significantly lower than the current cluster value. This is at odds with the recent spectroscopic measurements by Clementini et al. (2005) confirming that the RR Lyrae stars in NGC 6441 are metal-rich

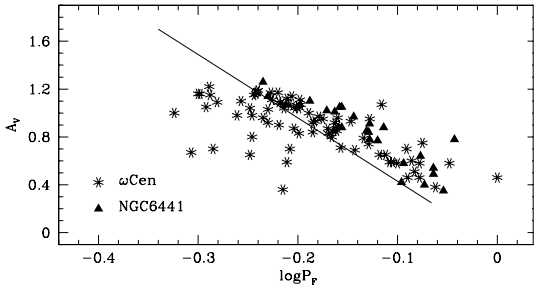

Fig. 6. Same as in Fig. 3, but for RR$_{ab}$ stars in the two peculiar clusters NGC 6441 (triangles) and ω Cen (asterisks).

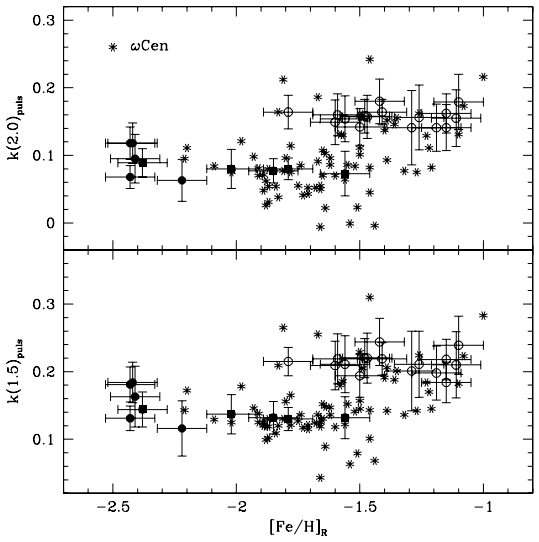

Fig. 7. The $k(1.5)_{\rm puls}$ (*bottom panel*) and the $k(2.0)_{\rm puls}$ (*top panel*) parameter for RR$_{ab}$ stars in ω Cen (asterisks) as a function of the metal abundance. Open circles, filled circles, and filled squares display Galactic globular clusters and have the same meaning as in Fig. 5.

with [Fe/H] $\sim -0.7 \pm 0.3$, on the Zinn & West (1984) scale (see also Gratton et al. 2007, and references therein).

On the other hand, if the NGC 6441 variables are generated by the very blue HB component, we should expect small $k_{\rm ev}$ values even with large metal abundances. However, even adopting HB $\sim +0.97$ the SHB simulations for $Z = 0.003$ and $Y \sim 0.25$ presented in Table 2 suggest $\langle k(1.5)_{\rm ev}\rangle \sim 0.15$ and $\langle k(2.0)_{\rm ev}\rangle \sim 0.14$ which are larger than the observed values. Since $k_{\rm ev}$ significantly depends on the pulsator luminosity, this discrepancy might imply a larger helium content, as recently suggested by Caloi & D'Antona (2007) who give $Y \sim 0.37$. However, star counts of HB and red giant branch stars in NGC 6441 provided by Layden et al. (1999) do not support the high helium abundance scenario. The new HB simulations with $Y = 0.30$ (Caputo et al. 2007, in preparation) and the modeling of the observed light curves (Clementini & Marconi 2007, in preparation) will probably shed new light on the unusual properties of the NGC 6441 RR Lyrae variables.

Regarding the variables in ω Cen, we plot in Fig. 7 the $k(1.5)_{\rm puls}$ and $k(2.0)_{\rm puls}$ values versus the [Fe/H]$_R$ metal abundance determined by Rey et al. (2000). We note again the quite large dispersion of the metallicity at constant $k_{\rm puls}$, thus stressing once more the misleading use of the Bailey diagram for reliable metal abundance determinations. The comparison with the Galactic globular cluster data presented in Fig. 5, here repeated for clarity, indicates that the bulk of RR$_{ab}$ stars in ω Cen behave

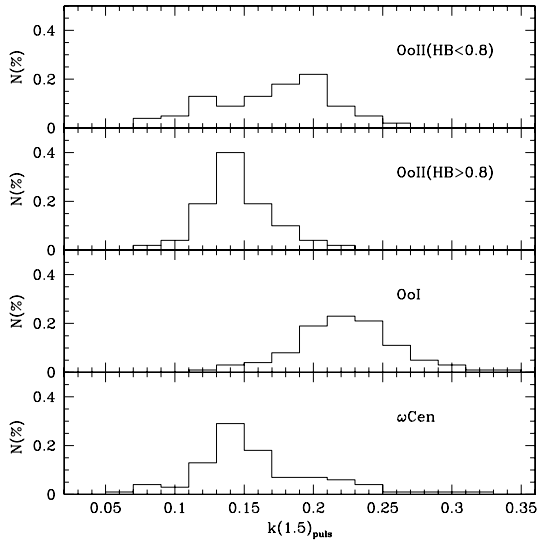

Fig. 8. Distribution of the $k(1.5)_{\rm puls}$ parameter for RR$_{ab}$ stars in ω Cen (*bottom panel*) together with OoI and OoII Galactic globular clusters.

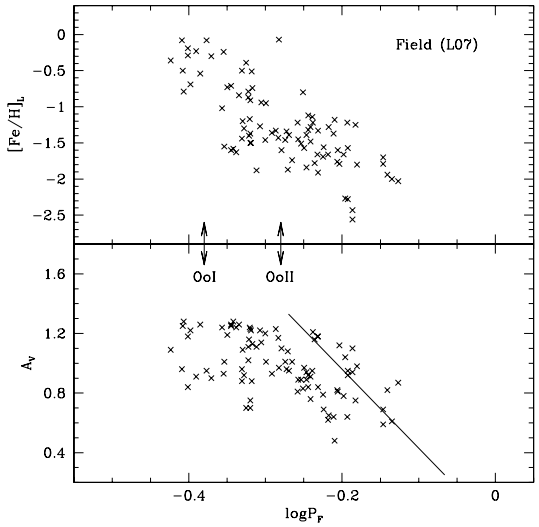

Fig. 9. RR$_{ab}$ stars in the solar neighborhood with measured [Fe/H] abundances (*top panel*; Layden 2007, private communication) and visual amplitudes (*bottom panel*; Nikolov et al. 1984). The arrows mark the shortest period observed in OoI and OoII Galactic globular clusters. The solid line shows the predicted ridge line for cluster OoII variables (see Fig. 3).

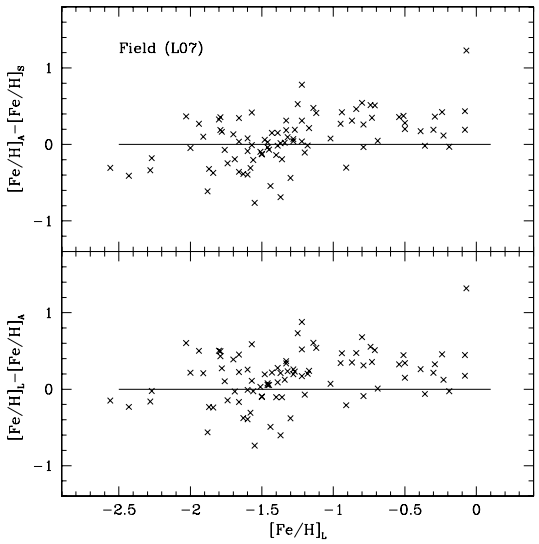

Fig. 10. Difference between the observed and the calculated [Fe/H] versus period for all the stars in Fig. 9.

as the variables in OoII clusters, with a minor fraction sharing the properties of the OoI variables (see also Clement & Rowe 2000). However, consistently with the ω Cen HB type, the agreement with the OoII group mainly applies to clusters not very metal-poor and with very blue HB morphology ([Fe/H] ≥ -2.2 and HB type $\geq$+0.8, filled squares) since the $k_{\rm puls}$ values typical of the variables observed in clusters with very low metal abundance and moderately blue HB morphology (e.g., M 15-like) seem to be absent. The lack of this type of variables shows up quite clearly from Fig. 8 which shows the frequency distribution of the $k(1.5)_{\rm puls}$ values in ω Cen (bottom) in comparison with those for OoI and OoII clusters. Note that this result, which holds also if the new metal abundances by Sollima et al. (2006) are adopted, cannot be explained by invoking a significant difference between the Kraft & Ivans (2003) and the Rey et al. (2000) metallicity scales. By using the Gratton et al. (2004) metal abundance [Fe/H]$_{\rm G}$ determinations for RR Lyrae stars in NGC 1851, NGC 3201, and in NGC 4590 we obtain [Fe/H]$_{\rm G}$ $\sim -0.48 + 0.65$[Fe/H]$_K$, while for ω Cen variables we derive [Fe/H]$_{\rm G}$ $\sim -0.41 + 0.71$[Fe/H]$_R$. Eventually, we find [Fe/H]$_K$ $\sim 0.1 + 1.1$[Fe/H]$_R$.

3.3. Field RR$_{ab}$ stars

Figure 9 shows the PA_V diagram of RR$_{ab}$ stars in the solar neighborhood for which [Fe/H] (Layden 1995, 1998, 2007, hereinafter [L07], private communication) and A_V data (Nikolov et al. 1984) are available. These stars are a mixture of OoII and OoI variables, with a further population at shorter periods than the OoI limit (see also the analysis of Kinemuchi et al. 2006, of a large sample of field variables.) and [Fe/H] ~ -0.5. As a first test, we show in Fig. 10 the difference between the measured metal content [Fe/H]$_L$ and the calculated values [Fe/H]$_A$ from Eq. (1) and [Fe/H]$_S$ from Eq. (2). In both cases, the average difference is $\sim\pm$0.3 dex, but the discrepancy for individual variables may be two or three times larger.

To repeat the procedure adopted for the variables in Galactic globular clusters, we have first verified that Eqs. (3) and (4) hold for fundamental RR Lyrae stars with $Z > 0.006$. As shown in Fig. 11, our pulsation models constructed by adopting $l/H_{\rm p} = 1.5$ and $Z = 0.01$, 0.02 (Bono et al. 1997) suggest that the constant term in Eq. (3) changes as $0.136 + 0.06(\log Z + 2.22)$. On these grounds, we determine the $k(1.5)_{\rm puls}$ values plotted in Fig. 12. A glance at the data plotted in this figure reveals three relevant points:

- the field stars, at constant $k_{\rm puls}$, show a dispersion in iron abundance that might reach $\pm$0.5 dex;
- the $k_{\rm puls}$ parameter steadly decreases, on average, when moving from [Fe/H]$\sim$ 0 to [Fe/H] ~ -2, but without any further decrease for the most metal-poor ([Fe/H] ~ -2.4) variables;
- the behavior of field stars and Galactic globular clusters, in the metallicity range [Fe/H] $= -1.0$ to -2.5, is quite similar. This finding supports the evidence for similar physical and evolutionary properties for field and cluster variables within this metallicity range.
- there is a significant difference between the RR$_{ab}$ variables in NGC 6441 and field variables with similar metal content.

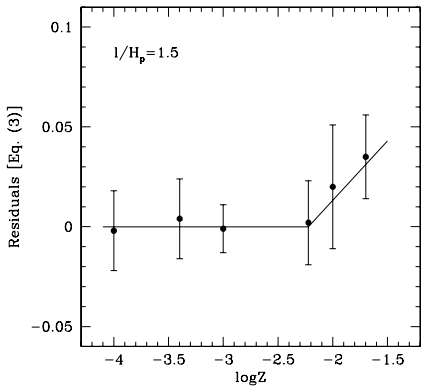

Fig. 11. Residuals to Eq. (3) for all the fundamental models from $Z = 0.0001$ to $Z = 0.02$.

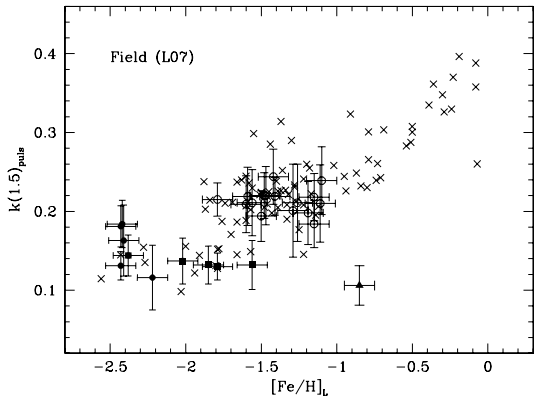

Fig. 12. Pulsational parameter $k(1.5)_{\rm puls}$ as a function of metal abundance $[{\rm Fe/H}]_L$ for all the field RR$_{ab}$ stars plotted in Fig. 9. The average values for Galactic globular clusters (symbols as in Fig. 5) and NGC 6441 (triangle) are also shown.

4. Exploiting the PA_V diagram

4.1. Period-Amplitude-Magnitude relation for RR$_{ab}$ stars

The circumstantial empirical and theoretical evidence discussed in the above sections brought into focus the deceptive use of the Bailey diagram of RR$_{ab}$ stars to estimate metal abundances. Therefore we now face the question: is there any possibility to exploit its dependence on the evolutionary status of the variables?

It is well known that current updated HB models provide, for fixed helium and metal content, slightly different luminosity values which are due to different assumptions concerning the input physics (see, e.g., Castellani 2003). On the contrary, the predicted mass of the RR Lyrae stars appears a more reliable parameter, with an average variation of ∼2% among the various evolutionary prescriptions available in the recent literature. It has already been shown in Paper II and Paper III that the coupling between the predicted relations inferred by the pulsation models, where mass and luminosity are free parameters, and the pulsator average mass suggested by SHB simulations provides a reliable "pulsational" route to the determination of the absolute magnitude of RR Lyrae stars *in globular clusters with known metal content and HB morphology*.

Then, we estimate the average mass of RR Lyrae stars in the selected globular clusters using the SHBs listed in Table 2, under the hypothesis of scaled-solar chemical compositions. In order to transform the measured [Fe/H] value into the global metallicity Z, we adopt the solar value $(Z/X)_\odot = 0.0245$ (Grevesse & Noels 1993) and $f = 1$ in the relation $\log Z = [{\rm Fe/H}] - 1.73 + \log(0.638f + 0.362)$, where f is the enhancement factor of α-elements with respect to iron (Salaris et al. 1993). The predicted mass values, which have an intrinsic uncertainty of ∼2%, are listed in Col. (4) of Table 5 and, once inserted into Eqs. (3) and (4), they provide the visual distance moduli $\mu_V^{k(1.5)}$ and $\mu_V^{k(2.0)}$ and the RR$_{ab}$ mean absolute magnitudes $\langle M_V^{k(1.5)}\rangle$ and $\langle M_V^{k(2.0}\rangle$ given in Cols. (5)−(8) in the same table.

Data plotted in Fig. 13, where for clarity the error bars are not drawn, show the direct consequence of the HB morphology-metallicity progression revealed in Fig. 2: the RR$_{ab}$ stars observed in OoII clusters with HB type bluer than +0.8 (filled squares) and in OoI clusters (open circles) obey a common relation between the absolute magnitude and the $k_{\rm puls}$ parameter, as given by

$$\langle M_V^{k(1.5)}\rangle = 0.12(\pm0.10) + 2.65(\pm0.07)\langle k(1.5)_{\rm puls}\rangle \quad (5)$$

and

$$\langle M_V^{k(2.0)}\rangle = 0.14(\pm0.10) + 2.67(\pm0.07)\langle k(2.0)_{\rm puls}\rangle, \quad (6)$$

while for the RR Lyrae variables in OoII clusters with moderately blue HB morphology (filled circles) the zero-points of the above relations (dashed lines) are moderately brighter by ∼0.05 mag.

Regarding the field RR Lyrae stars, we do not know the morphology of the parent HB star distribution, but luckily we can benefit from the well-known evidence that, for a fixed age, the predicted mass range of HB stars populating the RR Lyrae instability strip decreases with increasing the metal content. This is shown in Table 6, where the data already presented in Table 2 are implemented with new SHB results at $Y = 0.25$ (Caputo et al. 2007, in preparation) based on Pietrinferni et al. (2004, 2006) HB models produced by an RGB progenitor having an age of about 13 Gyr. Adopting $[{\rm Fe/H}] = 1.73 + \log Z$, a linear regression through the average values listed in the last column in this table gives

$$\langle \log M(RR)\rangle = -0.265 - 0.063[{\rm Fe/H}], \quad (7)$$

with the intrinsic uncertainty given by $\epsilon(\langle \log M({\rm RR})\rangle) = 0.005{-}0.02[{\rm Fe/H}]$. According to Eq. (3) and bearing in mind that with larger metal content than $Z = 0.006$ the constant term varies as $0.136 + 0.06(\log Z + 2.22)$, we eventually derive that the absolute magnitude of RR$_{ab}$ stars is given by

$$M_V^{k(1.5)} = 0.56 - 0.49A_V - 2.60\log P + 0.05[{\rm Fe/H}] \quad (8)$$

with $-1.0 \le [{\rm Fe/H}] \le -0.5$ and by

$$M_V^{k(1.5)} = 0.64 - 0.49A_V - 2.60\log P + 0.20[{\rm Fe/H}] \quad (9)$$

with $-0.5 \le [{\rm Fe/H}] \le 0$, with the magnitude total uncertainty varying as $\epsilon(M_V) = 0.07 - 0.02[{\rm Fe/H}]$.

4.2. M_V(RR)–[Fe/H] relation

Many calibrations of the RR Lyrae luminosity as a function of the metal content have been published in the literature (e.g., see Cacciari & Clementini 2003, for a summary) and the most recent suggest that the M_V(RR)–[Fe/H] is nonlinear for metal abundances ranging from [Fe/H] ∼ −0.5 to −2.4 (see Sandage 2006; Sandage & Tammann 2006, and references therein).

For our selected sample of Galactic globular clusters, Fig. 14 displays the PA_V-based mean absolute magnitude of RR$_{ab}$ stars

Table 5. Average mass M(RR) of RR$_{ab}$ stars in Galactic globular clusters inferred by SHB computations, adopting solar-scaled chemical compositions and $(Z/X)_{\odot} = 0.0245$. These masses are used with Eqs. (2) and (3) to estimate the visual distance moduli $\langle \mu_V \rangle$ and the mean absolute magnitudes $\langle M_V \rangle$ listed in Cols. (5)−(8).

Name	HB	[Fe/H]$_K$	M(RR)	$\mu_V^{k(1.5)}$	$\langle M_V^{k(1.5)} \rangle$	$\mu_V^{k(2.0)}$	$\langle M_V^{k(2.0)} \rangle$
Oosterhoff type II							
N4590	+0.44	−2.43	0.81	15.06 ± 0.09	0.54 ± 0.13	15.21 ± 0.09	0.39 ± 0.13
N6426	+0.58	−2.43	0.80	17.75 ± 0.07	0.42 ± 0.11	17.90 ± 0.06	0.27 ± 0.11
N7078	+0.67	−2.42	0.78	15.23 ± 0.08	0.57 ± 0.10	15.38 ± 0.08	0.41 ± 0.10
N5053	+0.52	−2.41	0.81	16.07 ± 0.10	0.50 ± 0.11	16.23 ± 0.10	0.34 ± 0.11
N6341	+0.91	−2.38	0.72	14.59 ± 0.09	0.48 ± 0.11	14.71 ± 0.08	0.36 ± 0.11
N5466	+0.58	−2.22	0.77	16.06 ± 0.09	0.40 ± 0.11	16.19 ± 0.07	0.27 ± 0.11
N5024	+0.81	−2.02	0.71	16.32 ± 0.07	0.47 ± 0.10	16.45 ± 0.06	0.34 ± 0.10
N6809	+0.87	−1.85	0.69	13.85 ± 0.07	0.47 ± 0.11	13.98 ± 0.05	0.35 ± 0.11
N6333	+0.87	−1.79	0.68	15.72 ± 0.06	0.47 ± 0.10	15.82 ± 0.05	0.36 ± 0.10
N7089	+0.96	−1.56	0.66	15.46 ± 0.09	0.48 ± 0.13	15.59 ± 0.09	0.36 ± 0.13
Oosterhoff type I							
N4147	+0.55	−1.79	0.71	16.24 ± 0.11	0.67 ± 0.14	16.35 ± 0.11	0.56 ± 0.14
I4499	+0.11	−1.60	0.70	16.99 ± 0.08	0.66 ± 0.10	17.13 ± 0.07	0.52 ± 0.10
N6934	+0.25	−1.59	0.70	16.19 ± 0.12	0.69 ± 0.12	16.32 ± 0.10	0.55 ± 0.12
N3201	+0.08	−1.56	0.70	14.08 ± 0.13	0.67 ± 0.13	14.21 ± 0.12	0.54 ± 0.12
N5272	+0.08	−1.50	0.69	15.00 ± 0.08	0.63 ± 0.10	15.12 ± 0.07	0.51 ± 0.10
N7006	−0.28	−1.48	0.70	18.11 ± 0.14	0.69 ± 0.15	18.24 ± 0.14	0.55 ± 0.15
N6715	+0.75	−1.47	0.67	17.38 ± 0.08	0.71 ± 0.11	17.52 ± 0.09	0.57 ± 0.11
N6981	+0.14	−1.42	0.68	16.10 ± 0.11	0.76 ± 0.15	16.24 ± 0.11	0.62 ± 0.15
N6229	+0.24	−1.41	0.68	17.35 ± 0.10	0.70 ± 0.13	17.47 ± 0.10	0.58 ± 0.13
N6864	−0.07	−1.29	0.67	17.02 ± 0.15	0.66 ± 0.16	17.15 ± 0.18	0.52 ± 0.16
N5904	+0.31	−1.26	0.66	14.38 ± 0.09	0.69 ± 0.13	14.50 ± 0.08	0.57 ± 0.13
N1851	−0.36	−1.19	0.66	15.40 ± 0.12	0.65 ± 0.12	15.52 ± 0.11	0.53 ± 0.12
N6121	−0.06	−1.15	0.66	12.73 ± 0.06	0.62 ± 0.10	12.82 ± 0.05	0.53 ± 0.10
N6362	−0.58	−1.15	0.66	14.56 ± 0.06	0.71 ± 0.10	14.68 ± 0.05	0.58 ± 0.10
N6723	−0.08	−1.11	0.65	14.68 ± 0.13	0.69 ± 0.16	14.80 ± 0.13	0.57 ± 0.16
N6171	−0.73	−1.10	0.65	14.91 ± 0.14	0.76 ± 0.15	15.04 ± 0.13	0.63 ± 0.15

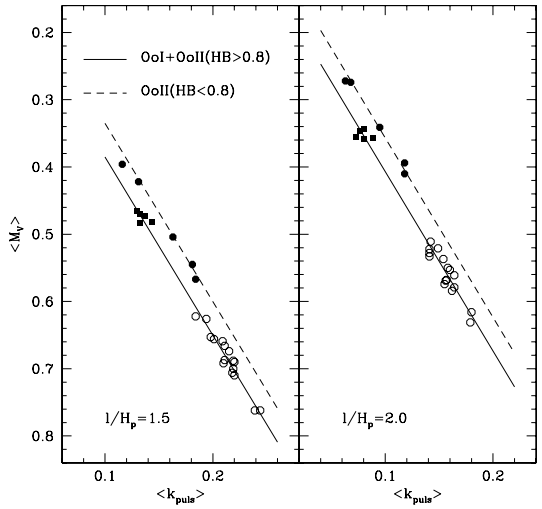

Fig. 13. *Left panel*: mean absolute magnitude of RR$_{ab}$ stars in Galactic globular clusters versus $\langle k_{\rm puls} \rangle$ for $l/H_{\rm p} = 1.5$ and by adopting scaled-solar chemical compositions and the solar ratio $(Z/X)_{\odot} = 0.0245$. The symbols are the same as in Fig. 5. The solid line is Eq. (5), while the dashed lines have a brighter zero-point (0.05 mag). *Right panel*: same as in the left panel, but with $l/H_{\rm p} = 2.0$. The solid line is Eq. (6).

(Cols. (6) and (8) in Table 5) versus the cluster metallicity [Fe/H]$_K$. The linear regression over the entire sample (solid line) yields a slope of 0.20 ± 0.06 mag dex^{-1}, regardless of the adopted mixing-length parameter, while the zero-point of the relation changes from 0.94 ± 0.10 mag to 0.82 ± 0.10 mag with $l/H_{\rm p} = 1.5$ and 2.0, respectively. However, the data given in Table 5 clearly show that at constant metal content the RR$_{ab}$ luminosity depends on the cluster HB type: e.g., the variables in NGC 7089 (HB = +0.96) are ∼0.2 mag brighter than those in IC 4499, NGC 6934 and NGC 3201, which show an HB type from HB = +0.08 to +0.25, yet all these clusters have nearly the same metallicity. This result is not new since theoretical (see Paper IV and references therein) and observational studies (Lee & Carney 1999; Clement & Shelton 1999; Alves et al. 2001) have already suggested that the RR Lyrae absolute magnitude depends on the cluster HB morphology and metal content.

The comparison with field RR$_{ab}$ stars with [Fe/H] ≥ −1.0 is shown in Fig. 15, where the absolute magnitudes of the field variables are determined by using Eqs. (8) and (9). It is quite clear that the linear M_V(RR)-[Fe/H] relation provided by Galactic globular clusters is not suitable for the most metal-rich ([Fe/H] ≥ −0.7) field variables. Conversely, we show in Fig. 16 that over the whole metallicity range of [Fe/H] = −2.5 to ∼0 *all* the variables are well fitted by the quadratic relation

$$M_V^{k(1.5)} = 1.19(\pm 0.10) + 0.50[\mathrm{Fe/H}] + 0.09[\mathrm{Fe/H}]^2. \quad (10)$$

4.3. What value of the mixing length parameter?

We have shown that the value of the mixing length parameter influences the zero-point of the Period-Amplitude-Magnitude relation (Eqs. (5) and (6)) and consequently the M_V(RR)-[Fe/H] calibration (see Fig. 14).

In order to constrain the most appropriate value of the mixing-length parameter for globular cluster RR$_{ab}$ stars, we show in Fig. 17 the V_0 magnitudes of RR$_{ab}$ stars in ω Cen

Table 6. Selected results of SHB simulations with $Z \geq 0.002$. For each given metal abundance, we list the mean mass of HB stars producing very blue and very red HB types and the corresponding mean mass of RR Lyrae stars. The last column gives the average mass (logarithm) of the predicted RR Lyrae stars for the whole range from HB = +0.95 to HB = −0.95. All the mass values hold for old stellar structures (see text).

Z	[Fe/H]	$\langle M(\mathrm{HB})\rangle$ HB = +0.95	$\langle M(\mathrm{RR})\rangle$ HB = +0.95	$\langle M(\mathrm{HB})\rangle$ HB = −0.95	$\langle M(\mathrm{RR})\rangle$ HB = −0.95	$\langle \log M(\mathrm{RR})\rangle$
0.002	−0.96	0.58	0.62 ± 0.02	0.69	0.65 ± 0.03	−0.200 ± 0.024
0.003	−0.79	0.56	0.60 ± 0.02	0.66	0.62 ± 0.03	−0.217 ± 0.021
0.004	−0.66	0.55	0.59 ± 0.02	0.65	0.61 ± 0.02	−0.225 ± 0.013
0.006	−0.49	0.54	0.58 ± 0.02	0.64	0.59 ± 0.02	−0.234 ± 0.010
0.008	−0.37	0.53	0.56 ± 0.01	0.63	0.58 ± 0.01	−0.245 ± 0.008
0.01	−0.27	0.52	0.56 ± 0.01	0.62	0.57 ± 0.01	−0.249 ± 0.007
0.02	+0.03	0.51	0.54 ± 0.01	0.58	0.55 ± 0.01	−0.264 ± 0.005

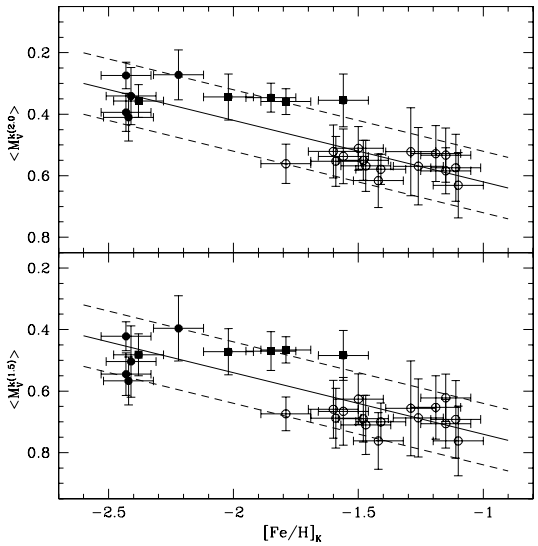

Fig. 14. Mean absolute visual magnitudes $\langle M_V^{k(1.5)}\rangle$ (*bottom panel*) and $\langle M_V^{k(2.0}\rangle$ (*top panel*) of RR$_{ab}$ stars in Galactic globular clusters versus [Fe/H]$_K$, according to scaled-solar chemical compositions and a solar ratio $(Z/X)_\odot = 0.0245$. The symbols are the same as in Fig. 5. The solid line shows the linear regression through the entire sample and has a slope of 0.20 mag dex^{-1}, while the dashed lines show the 1σ uncertainty. See text for more details.

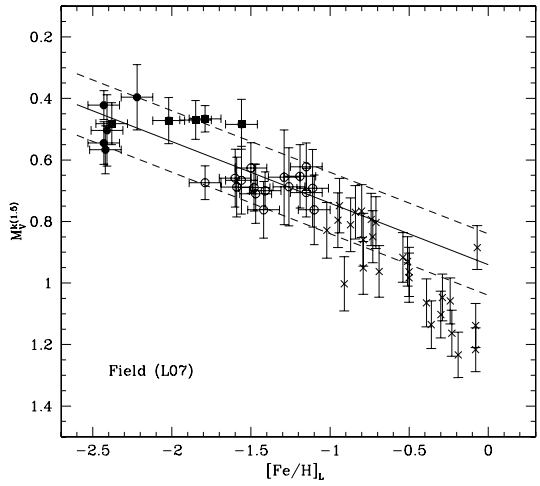

Fig. 15. Absolute visual magnitudes $M_V^{k(1.5)}$ versus [Fe/H]$_L$ for field RR$_{ab}$ stars more metal-rich than [Fe/H]$_L = -1.0$ in comparison with Galactic globular cluster variables. Symbols and lines are the same as in the bottom panel of Fig. 14.

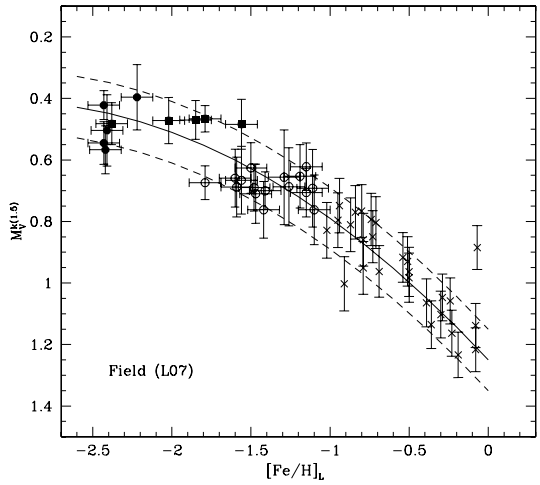

Fig. 16. Same as Fig. 14, but with cluster and field data fitted with a quadratic relation.

(Piersimoni et al. 2007, in preparation) versus the observed $k(1.5)_{\mathrm{puls}}$ and $k(2.0)_{\mathrm{puls}}$ parameters. By using Eqs. (5) and (6), we find a cluster intrinsic distance modulus of $\mu_0 = 13.68 \pm 0.10$ mag and 13.80 ± 0.10 mag, respectively. Unfortunately, both these estimates agree within 1σ with the distance $\mu_0 = 13.75 \pm 0.04$ mag based on the eclipsing binary OGLEGC-17 (Thompson et al. 2001; Kaluzny et al. 2002). Therefore, we decided to consider a further pulsational method, namely the FOBE method (Caputo 1997; Caputo et al. 2000) which provides the cluster apparent distance modulus by matching the observed distribution of the RR$_c$ variables in the V–log P plane with the predicted blue (hot) edge of the first-overtone instability region. The reason for this choice is that the FOBE-based distance modulus μ_V(FOBE) is expected to decrease with increasing the mixing-length parameter (see Eq. (2) in Paper III), at variance with the apparent distance $\mu_V(PA_V)$ inferred from the PA_V relation.

Figure 18 shows the comparison between the two sets of distance moduli. We find that for $l/H_{\mathrm{p}} = 1.5$ the μ_V(FOBE) distances are on average larger than those based on $\mu_V(PA_V)$, whereas the opposite applies for $l/H_{\mathrm{p}} = 2.0$. This evidence indicates that we can adopt $l/H_{\mathrm{p}} \sim 1.7$, although the best solution discussed in Paper III is probably given by a mixing-length parameter that slightly increases when moving from the blue to the red side of the instability strip, i.e., from *c*- to *ab*-type variables. The very recent investigation by Ferraro et al. (2006) on red giant stars in globular clusters supports a value $l/H_{\mathrm{p}} = 2.0$ for these cool stars and a negligible dependence on metallicity.

The use of different scalings between the iron abundance and the global metallicity (Z–[Fe/H]) has marginal effects on

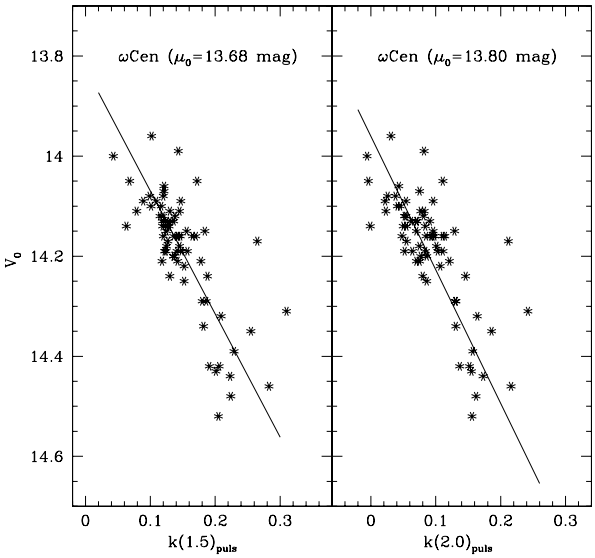

Fig. 17. Unreddened visual magnitude V_0 of RR$_{ab}$ stars in ω Cen plotted versus $k(1.5)_{\rm puls}$ and $k(2.0)_{\rm puls}$. The solid line plotted in the left panel refers to Eq. (5) and accounts for an intrinsic distance modulus μ_0 = 13.68 mag. The solid line plotted in the right panel refers to Eq. (6) and accounts for μ_0 = 13.80 mag.

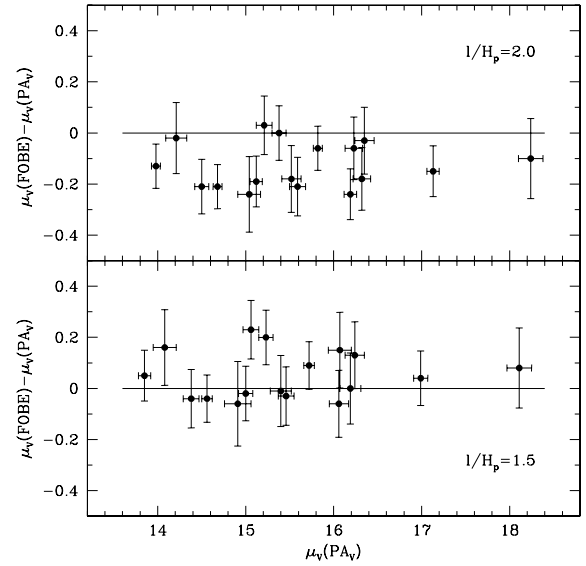

Fig. 18. Comparison between the apparent distance moduli of RR$_c$ variables based on the FOBE method and the RR$_{ab}$ distance moduli based on the PA_V relation for the two adopted values of the mixing-length parameter. The data refer to scaled-solar chemical compositions and to the solar ratio $(Z/X)_\odot$ = 0.0245.

the RR$_{ab}$ absolute magnitudes listed in Table 5. By adopting f = 3 ([α/Fe] ∼ 0.5) with $(Z/X)_\odot$ = 0.0245 yields, at fixed [Fe/H], smaller masses by ∼6%, and in turn fainter absolute magnitudes by ∼0.03 mag, when compared with the values listed in Table 5. The dependence on the adopted solar ratio is even smaller, and indeed by adopting $(Z/X)_\odot$ = 0.0165 (Asplund et al. 2004), the mass and magnitude variations for f = 1 are only ∼+3% and −0.01 mag, while for f = 3 we estimate ∼−3% and ∼+0.01 mag, respectively.

5. Conclusions and final remarks

Hydrodynamical models of fundamental RR Lyrae stars computed by adopting a metal content from Z = 0.0001 to 0.006 and two different values of the mixing-length parameter ($l/H_{\rm p}$ = 1.5 and 2.0) provide detailed predictions concerning the pulsation parameters connecting the period with the V-band amplitude. In order to investigate the distribution of cluster RR$_{ab}$ stars in the PA_V diagram, we consider the following pulsational parameters

$$k(1.5)_{\rm puls} = 0.13 - \log P_{ab} - 0.189 A_V$$

and

$$k(2.0)_{\rm puls} = 0.03 - \log P_{ab} - 0.142 A_V,$$

and we find that the average values $\langle k(1.5)_{\rm puls}\rangle$ and $\langle k(2.0)_{\rm puls}\rangle$ do not show significant changes among OoI clusters with metal abundances ranging from [Fe/H] = −1.8 to −1.1 and intermediate to red HB types. On the other hand, the same parameters present a mild decrease among the OoII clusters with very blue HB types, even if these clusters are also the less metal-poor of the group. Moreover, in the relatively narrow metallicity range [Fe/H] = −1.7 ± 0.1, where both OoI and OoII clusters are observed, the former clusters have redder HB types *and* larger $\langle k_{\rm puls}\rangle$ values than the latter ones.

A linear fit over the entire sample of globular clusters yields a [Fe/H]-$k_{\rm puls}$ relation with a large intrinsic dispersion of ≈0.4 dex. The dispersion becomes even larger if the calibration relies on selected clusters: if we adopt a mix of OoI and OoII clusters with moderately blue HB morphology, then the metal abundance of RR$_{ab}$ in clusters characterized by a very blue HB morphology will be underestimated by ≈0.7 dex, whereas if we adopt a mix of OoI and OoII clusters with very blue HB morphologies the metallicity of RR$_{ab}$ in clusters characterized by a moderately blue HB morphology will be overestimated by ≈0.5 dex. This circumstantial evidence casts doubt on the use of the PA_V distribution of RR$_{ab}$ variables as a diagnostic of the metal abundance. This finding is independently supported by the sizable samples of RR$_{ab}$ variables in ω Cen and in the solar neighborhood for which metal abundance and V-band amplitudes are available. The distribution of these objects in the PA_V plane shows that the spread in metal abundance, at constant $k_{\rm puls}$, is of the order of 0.5 dex.

By coupling pulsation models and synthetic horizontal branch simulations, we show that the pulsation parameter $k_{\rm puls}$ is a reliable distance indicator for globular clusters with known metal content and HB type. The occurrence of a Period-Luminosity-Amplitude relation for RR$_{ab}$ stars was originally suggested by Sandage (1981a,b) and that the present use of detailed evolutionary and pulsational predictions provides the opportunity to constrain the dependence on the globular cluster HB type and metal content. We find that the RR$_{ab}$ in OoI clusters and in OoII clusters with HB types bluer than +0.8 do obey a well defined M_V-$k_{\rm puls}$ relations. In particular, we find

$$\langle M_V^{k(1.5)}\rangle = 0.12(\pm0.09) + 2.65(\pm0.07)\langle k(1.5)_{\rm puls}\rangle$$

and

$$\langle M_V^{k(2.0)}\rangle = 0.14(\pm0.09) + 2.67(\pm0.07)\langle k(2.0)_{\rm puls}\rangle,$$

while the RR$_{ab}$ in OoII clusters with moderately blue HB morphology present, at fixed $k_{\rm puls}$, a zero-point that is ∼0.05 mag

brighter. Regarding the variables in the solar neighborhood, additional pulsation models with $l/H_{\rm p} = 1.5$ and $Z > 0.006$ together with the predicted metallicity dependence of the mass of metal-rich ([Fe/H] ≥ -1.0) RR Lyrae stars

$$\langle \log M(RR) \rangle = -0.265 - 0.063[{\rm Fe/H}]$$

yield

$$M_V^{k(1.5)} = 0.56 - 0.49A_V - 2.60 \log P + 0.05[{\rm Fe/H}]$$

with $-1.0 \leq$ [Fe/H] ≤ -0.5 and

$$M_V^{k(1.5)} = 0.64 - 0.49A_V - 2.60 \log P + 0.20[{\rm Fe/H}]$$

with $-0.5 \leq$[Fe/H] ≤ 0.

Once the PA_V-based absolute magnitude M_V(RR) is derived, the resulting correlation with the globular cluster metallicity $[{\rm Fe/H}]_K$ has a slope of 0.20 ± 0.06 mag dex^{-1}, regardless of the adopted mixing-length parameter, while the zero-point changes from 0.94 ± 0.10 to 0.82 ± 0.10 mag when using pulsation models constructed by assuming a mixing length parameter $l/H_{\rm p} = 1.5$ and $l/H_{\rm p} = 2.0$, respectively. However, the inclusion of the metal-rich field variables yields that over the total metallicity range from [Fe/H] $= -2.5$ to $\sim$0 the relation becomes quadratic as

$$M_V^{k(1.5)} = 1.19(\pm 0.10) + 0.50[{\rm Fe/H}] + 0.09[{\rm Fe/H}]^2$$

in agreement with the results presented by Bono et al. (2003) and Sandage (2006).

Finally, in order to constrain the most appropriate value of the mixing-length parameter, we adopt the RR$_{ab}$ stars in ω Cen, but the PA_V-based true distance moduli, $\mu_0 = 13.68 \pm 0.09$ mag for $l/H_{\rm p} = 1.5$ and 13.80 ± 0.09 mag for $l/H_{\rm p} = 2.0$, agree within 1σ with the distance $\mu_0 = 13.75 \pm 0.04$ mag based on the eclipsing binary OGLEGC-17 (Thompson et al. 2001; Kaluzny et al. 2002). Therefore, we adopt the FOBE method that provides cluster apparent distance moduli which decrease with increasing the mixing-length parameter. We find that distance estimates based on the PA_V and on the FOBE method agree for an intermediate mixing-length parameter, namely $l/H_{\rm p} \sim 1.7$.

Acknowledgements. It is a real pleasure to thank H. Smith for several suggestions and a detailed reading of an early draft of this paper. We also warmly thank A. Layden for his valuable data on field RR Lyrae stars and his helpful comments. We also acknowledge the anonymous referee for his/her positive comments and suggestions that helped us to improve the readability of the manuscript. This work was partially supported by PRIN-INAF2005 (P.I.: A. Buzzoni), "Galactic Stellar Populations", by PRIN-INAF2004 (P.I.: M. Bellazzini), "A hierarchical merging tale told by stars: motions, ages and chemical compositions within structures and substructures of the Milky Way".

References

Alcock, C., Allsman, R. A., Alves, D. R., et al. 2000, AJ, 119, 2194
Alves, D. R., Bond, H. E., & Onken, C. 2001, AJ, 121, 318
Asplund, M., Grevesse, N., Sauval, A. J., Allende Prieto, C., & Kiselman, D. 2004, A&A, 417, 751
Bono, G., Caputo, F., Cassisi, S., Incerpi, R., & Marconi, M. 1997, ApJ, 483, 811
Bono, G., Caputo, F., Castellani, V., et al. 2003, MNRAS, 344, 1097
Brown, T. M., Ferguson, H. C., Smith, E., et al. 2004, AJ, 127, 2738
Cacciari, C., & Clementini, G. 2003, in Stellar Candles for the Extragalactic Distance Scale, ed. D. Alloin, & W. Gieren (Berlin: Springer-Verlag), LNP, 635, 105
Caloi, V., & D'Antona, F. 2007, A&A, 463, 949
Caputo, F. 1997, MNRAS, 284, 994
Caputo, F., Castellani, V., Marconi, M., & Ripepi, V. 2000, MNRAS, 316, 819
Cassisi, S., Castellani, M., Caputo, F., & Castellani, V. 2004, A&A, 426, 641 (Paper IV)
Castellani, V. 2003, in New Horizons in Globular Cluster Astronomy, ed. G. Piotto, G. Meylan, S. G. Djorgovski, & M. Riello (San Francisco: ASP), 159
Castelli, F., Gratton, R. G., & Kurucz, R. L. 1997a, A&A, 318, 841
Castelli, F., Gratton, R. G., & Kurucz, R. L. 1997b, A&A, 324, 432
Catelan, M. 2005, in Resolved Stellar Populations, ed. D. Valls-Gabaud, & M. Chavez (San Francisco, ASP), 123
Catelan, M., Pritzl, B. J., & Smith, H. A. 2004, ApJS, 154, 633
Clementini, G., Ripepi, V., Bragaglia, A., et al. 2005, MNRAS, 363, 734
Ferraro, F. R., Valenti, E., Straniero, O., & Origlia, L. 2006, ApJ, 642, 225
Clement, C. M., & Rowe, J. 2000, AJ, 120, 2579
Clement, C. M., & Shelton, I. 1999, ApJ, 515, L85
Demarque, P., Zinn, R., Lee, Y.-W., & Yi, S. 2000, AJ, 119, 1398
Di Criscienzo, M., Marconi, M., & Caputo, F. 2004, ApJ, 612, 1092 (Paper III)
Di Criscienzo, M., Caputo, F., Marconi, M., & Musella, I. 2006, MNRAS, 365, 1357
Gratton, R. G., Bragaglia, A., Clementini, G., et al. 2004, A&A, 421, 937
Gratton, R. G., Lucatello, S., Bragaglia, A., et al. 2007, A&A, 464, 953
Grevesse, N., & Noels, A. 1993, Phys. Scr., T47, 133
Harris, W. E. 1996, AJ, 112, 1487
Kaluzny, J., Thompson, I., Krzeminski, W., et al. 2002, in ω Cen, a Unique Window into Astrophysics, ed. F. van Leeuwen, J. D. Hughes, & G. Piotto (San Francisco: ASP), 155
Kinemuchi, K., Smith, H. A., Wozniak, P. R., & McKay, T. A. 2006, AJ, 132, 1202
Kraft, R. P., & Ivans, I. I. 2003, PASP, 115, 143
Layden, A. C. 1995, AJ, 110, 2312
Layden, A. C. 1998, AJ, 115, 193
Layden, A. C., Ritter, L. A., Welch, D. L., & Webb, T. M. A. 1999, AJ, 117, 1313
Lee, Y.-W. 1990, ApJ, 363, 159
Lee, J.-W., & Carney, B. W. 1999, AJ, 118, 1373
Marconi, M., Caputo, F., Di Criscienzo, M., & Castellani, M. 2003, ApJ, 596, 299 (Paper II)
Nikolov, N., Buchantsova, N., & Frolov, M. 1984, The Mean Light and Color ($B-V$ and $U-B$) of 210 Field RR Lyrae Type Stars (Sofia: Astron. Council USSR Acad. Sci.)
Pietrinferni, A., Cassisi, S., Salaris, M., & Castelli, F. 2004, ApJ, 612, 168
Pietrinferni, A., Cassisi, S., Salaris, M., & Castelli, F. 2006, ApJ, 642, 797
Preston, G. W. 1959, ApJ, 130, 507
Pritzl, B. J., Smith, H. A., Catelan, M., & Sweigart, A. V. 2001, AJ, 122, 2600
Rey, S.-C., Lee, Y.-W., Joo, J.-M., Walker, A. R., & Baird, S. 2000, AJ, 119, 1824
Rich, R. M., et al. 1997, ApJ, 484, L25
Salaris, M., Chieffi, A., & Straniero, O. 1993, ApJ, 414, 580
Sandage, A. 1981a, ApJ, 244, L23
Sandage, A. 1981b, ApJ, 248, 161
Sandage, A. 2004, AJ, 128, 858
Sandage, A. 2006, AJ, 131, 1750
Sandage, A., & Tammann, G. A. 2006, ARA&A, 44, 93
Sollima, A., Borissova, J., Catelan, M., et al. 2006, ApJ, 640, L43
Stellingwerf, R. F. 1984, ApJ, 284, 712
Thompson, I. B., Kaluzny, J., Pych, W., et al. 2001, AJ, 121, 3089
van Albada, T. S., & Baker, N. 1971, ApJ, 169, 311
van Albada, T. S., & Baker, N. 1973, ApJ, 185, 477
Zinn, R., & West, M. J. 1984, ApJS, 55, 45